



CHORUS

This is the accepted manuscript made available via CHORUS. The article has been published as:

Domain size criterion for the observation of all-optical helicity-dependent switching in magnetic thin films

Mohammed Salah El Hadri, Michel Hehn, Philipp Pirro, Charles-Henri Lambert, Grégory Malinowski, Eric E. Fullerton, and Stéphane Mangin

Phys. Rev. B **94**, 064419 — Published 15 August 2016

DOI: [10.1103/PhysRevB.94.064419](https://doi.org/10.1103/PhysRevB.94.064419)

Domain size criterion for the observation of all-optical helicity-dependent switching in magnetic thin films

Mohammed Salah El Hadri,^{1,*} Michel Hehn,¹ Philipp Pirro,¹ Charles-Henri Lambert,¹ Grégory Malinowski,¹ Eric E. Fullerton,² and Stéphane Mangin¹

¹*Institut Jean Lamour, UMR CNRS 7198, Université de Lorraine, BP 70239, F-54506, Vandoeuvre-lès-Nancy, France*

²*Center for Magnetic Recording Research, University of California San Diego, La Jolla, CA 92093-0401, USA*

(Dated: July 29, 2016)

To understand the necessary condition for the observation of all-optical helicity-dependent switching (AO-HDS) of magnetization in thin films, we investigated ferromagnetic Co/Pt and Co/Ni multilayers as well as ferrimagnetic TbCo alloys as a function of magnetic layer compositions and thicknesses. We show that both ferro- and ferri-magnets with high saturation magnetization show AO-HDS if their magnetic thickness is strongly reduced below a material-dependent threshold thickness. By taking into account the demagnetizing energy and the domain wall energy, we are able to define a criterion to predict whether AO-HDS or thermal demagnetization (TD) will be observed. This criterion for the observation of AO-HDS is that the equilibrium size of magnetic domains forming during the cooling process should be larger than the laser spot size. From these results we anticipate that more magnetic materials are expected to show AO-HDS. However, the effect of the optical pulses' helicity is hidden by the formation of small magnetic domains during the cooling process.

I. INTRODUCTION

Understanding the interaction between ultrashort laser pulses and magnetization became a topic of great interest, since the first observation of ultrafast demagnetization in Ni thin films arising from a single laser pulse by Beaurepaire *et al.* [1]. In 2007, a fascinating discovery related to ultrafast demagnetization was the observation of all-optical switching (AOS) of magnetization using only ultrashort laser pulses [2]. Indeed, cutting-edge experiments have demonstrated the ability to switch the magnetization of ferrimagnetic GdFeCo films using femtosecond laser pulses without any external magnetic field [2, 3]. Under the action of a single fs laser pulse, the AOS of GdFeCo films is shown to be ultrafast, occurring on a picosecond timescale [4]. Moreover, the AOS has been described as a purely thermal process [5] and is attributed to the distinct dynamics of Gd and FeCo sublattices leading to a transient ferromagnetic like state [4]. The all-optical helicity-dependent switching (AO-HDS) of GdFeCo films was obtained only with multiple-pulse exposure [2] and for a narrow range of fluence, which was explained by magnetic circular dichroism [6]. Later, all-optical switching was demonstrated in a much larger variety of ferrimagnetic materials, such as ferrimagnetic alloys with different rare-earth (RE) namely Tb, Dy and Ho [7, 8], ferrimagnetic multilayers and free-RE synthetic ferrimagnets [8]. This AOS was helicity-dependent for a wide range of fluences ranging from the switching threshold to the damage threshold [8].

Several models and experimental conditions have been proposed to elucidate the AO-HDS in ferrimagnetic ma-

terials building on the experimental finding for ferrimagnetic GdFeCo. In this context, it was first proposed that an antiferromagnetic exchange coupling between non-equivalent sublattices is required to achieve the AO-HDS in ferrimagnets [9]. Later, it was also reported that there is a low remanence criterion for AO-HDS in various ferrimagnetic materials [10]. AO-HDS was only obtained for a remanence below a threshold of 220 emu/cm³ [10, 11]. Nevertheless, the recent discovery of AO-HDS in several pure ferromagnetic films and granular media [12, 13] strongly challenges the proposed parameters ruling the achievement of AO-HDS, since these ferromagnetic materials do not possess an antiferromagnetic coupling between two sublattices, and have a magnetization far above the proposed remanence threshold. Here, we present a comprehensive investigation of the magnetic parameters needed to observe AO-HDS in ferrimagnetic TbCo alloys and ferromagnetic Co/Ni and Co/Pt multilayers for a wide range of compositions and thicknesses. This investigation highlights the role of the magnetic film thickness for the successful observation of the AO-HDS. We can prove that ferrimagnetic TbCo alloys showing only laser induced demagnetization effects for high thicknesses demonstrate AO-HDS if their thickness is drastically scaled down, and even with saturation magnetization as well as a remanence in the vicinity of 830 emu/cm³. We also reveal that ferromagnetic multilayers with a saturation magnetization of 1480 emu/cm³ demonstrate AO-HDS if their thickness is sufficiently low. These findings demonstrate that the demagnetizing energy gain by forming magnetic domains and hence the size of stable domains play a decisive role in the helicity-dependent laser-induced switching as was speculated in Lambert *et al.* [12].

* mohammed-salah.elhadri@univ-lorraine.fr

II. SAMPLES STRUCTURE AND CHARACTERIZATION

To explore the influence of different magnetic parameters on the observation of AO-HDS, we study various ferrimagnetic and ferromagnetic thin films of different thicknesses. All these films were grown by DC magnetic sputtering, and show a strong perpendicular magnetic anisotropy (PMA) leading to a perpendicular to film plane magnetization at remanence. The direction of the easy axis, the saturation magnetization and the coercive field are determined using SQUID magnetometry. The investigated ferrimagnetic thin films are composed of Glass/Ta(3 nm)/Pt(5 nm)/Tb_xCo_{1-x} (t)/Pt(5 nm), in which the RE (Tb) and TM (Co) magnetic moments are antiferromagnetically coupled. The top Pt layer prevents sample oxidation. The net magnetization of the alloy is given by the sum of the magnetization of the RE and the TM sublattices. Consequently, for a given temperature the net magnetization can be equal to zero at a given RE concentration (x_{comp}). For larger (resp. lower) RE concentration, the magnetization will be pointing along the RE (resp. TM) moments and the net magnetization will be named “RE dominant” (resp. “TM dominant”). In our case, the Tb atomic concentration x in the alloy is ranging from 8 at.% to 30 at.% with an alloy thickness t ranging from 1.5 to 20 nm. At room temperature (RT) and for a thickness of 20 nm, a transition from a Tb dominant to Co dominant ferrimagnet is taking place if x is decreased below 20 at.% (i.e. x_{comp} (300 K) = 20%) [7].

One issue that we faced is that once the sample thickness is strongly reduced, the nominal concentration x_{nom} varies from the effective concentration x determined by the deposition. As previously reported for other ferrimagnetic materials [11, 14, 15], the composition x at which this crossover occurs depends on thickness. To explain such behavior, several mechanisms have been reported in the literature. In [14, 15], this behavior was related to the diffusion of the RE atoms and a segregation process that can take place causing a deviation of the Tb concentration in the studied films. This effect is particularly pronounced for low thicknesses because of the high surface to volume ratio. In [11], the compensation point and the remanent magnetization of TbFe alloys films was related to a growth-induced modification of the microstructure of the amorphous films, which affects the short range order. As a result, the sperimagnetic cone angle of the Tb atoms changes and leads to a change of saturation magnetization. Similar effects occur in our TbCo alloy thin films. In order to simplify the discussion, we decided here to report the Tb concentration x which corresponds to the effective concentration. This concentration is deduced from the saturation magnetization M_s and compared with the one measured on thicker films presented in [7]. Since CoTb alloy is sandwiched between Pt layers, we neglected any dead layer at the CoTb/Pt interface and also neglected the possible Pt polarization induced by the CoTb layer.

Two different ferromagnetic multilayer thin film systems were investigated, namely Glass/Ta(3 nm)/Pt(3 nm)/[Pt(0.7 nm)/Co(0.6 nm)]_N/Pt(3.7 nm) multilayers and Glass/Ta(3 nm)/Cu/[Co(0.2 nm)/Ni(0.6 nm)]_N/Cu/Pt(3 nm) multilayers, where the top Pt layer prevents sample oxidation. The Cu(111) base layer promotes the PMA of [Co/Ni]_N multilayers [16], whereas the Cu capping layer decouples the [Co/Ni]_N stack from the top Pt layer. The number of repeats N is varying from 1 to 4 for Co/Pt multilayers and from 2 to 6 for Co/Ni multilayers. All these ferromagnetic multilayer thin films present a perpendicular anisotropy leading to perpendicular magnetization at room temperature. The saturation magnetization of [Co/Pt]_N multilayers varies from 1483, 1609, 2194 to 2217 emu/cm³ for $N = 1, 2, 3$ and 4, respectively. This increase of the saturation magnetization with the number of repeats N is attributed to the spin polarization of Pt atoms at the interfaces by the adjacent Co layers [17]. Note that the thickness of the spin polarized Pt is not taken into account for the calculation of the saturation magnetization. Furthermore, the investigated [Co/Ni]_N multilayers show a saturation magnetization $M_s = 1100$ emu/cm³ and changes only weakly with the number of repeats.

For AO-HDS experiments we used a Ti: sapphire fs-laser with a 5-kHz repetition rate, a wavelength of 800 nm (1.55 eV), and a pulse duration of 35 fs. The Gaussian beam spot is focused with a FWHM of approximately 50 μ m. A quarter-wave plate is used to transform the linearly polarized beam (π) into right- ($\sigma+$) and left- ($\sigma-$) handed circularly polarized beam, whereas the laser power is adjusted using a half-wave plate. The samples are excited through the glass substrate with laser powers ranging from 0.5 mW for films with lower thicknesses up to 3 mW for films with larger thicknesses. Note that the AO-HDS ability of the investigated films is found to be maintained for a laser power ranging from the threshold below which the laser does not affect the magnetization to the damage threshold [8, 12, 18]. The response of the investigated magnetic films is probed using static Faraday microscope in order to image the magnetic domains in transmission. The circularly polarized beam is swept over the magnetic films with a sweeping speed of 10 μ m/s and then the film is imaged to determine the final magnetic state. If the final magnetic state is uniform in the area irradiated by the laser and is dependent on the helicity of the light, we consider this AO-HDS. On the other hand, if the final state is multiple magnetic domains and independent of the helicity we characterize this as thermal demagnetization (TD).

III. RESULTS AND DISCUSSION

A. Thickness-dependence of all-optical switching in ferrimagnetic Tb-Co films

We investigated AO-HDS in $\text{Tb}_x\text{Co}_{1-x}$ (t) alloy films for a large range of magnetic thickness t and Tb concentration x . Two nominal concentrations of Tb (16% and 30%) have been used. By varying t from 1.5 nm to 20 nm, Tb concentration x varies from 8 at.% to 30 at.% due to the thickness effect discussed previously (see Supplemental Fig. 1). Prior to being optically excited, the thin films are saturated with an external magnetic field applied perpendicular to film plane, whereas no magnetic field is applied during the optical excitation. The fs laser beam is then swept from right to left for both right- ($\sigma+$) and left- ($\sigma-$) circular polarization. Note that the magneto-optical Faraday microscopy is mainly sensitive to the perpendicular component of the Co sublattice magnetization. Therefore, after initial magnetization saturation up, the contrast corresponding to a reversal to down is dark (resp. white) for Co dominant (resp. Tb dominant) TbCo alloy films (see Figs. 1 and 2).

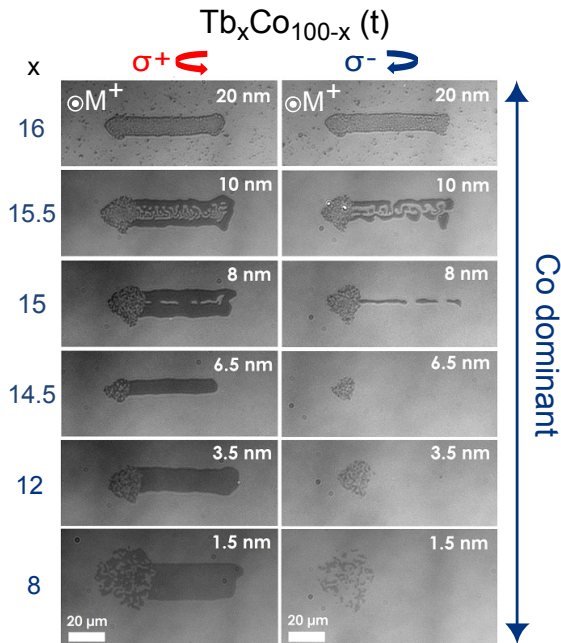


FIG. 1. Faraday imaging of $\text{Tb}_x\text{Co}_{100-x}$ (t) alloy films for Tb concentration x ranging from 8 to 16 and alloy thickness varying from 1.5 nm to 20 nm. For each sample, right- and left-circularly polarized laser beam were swept over the sample from right to left. The initial magnetization saturation up is exemplarily shown. The dark contrast corresponds to a reversal to down. The laser power is ranging from 1.15 mW (for $t < 8$ nm) to 1.5 mW (for $t > 8$ nm).

For a large thickness $t = 20$ nm, one can see in Figs. 1 and 2 that thermal demagnetization (TD) is obtained

for $x = 16$ at.% (Fig. 1) while AO-HDS is obtained for $x = 30$ at.% (Fig. 2), which is in agreement with previous studies [7, 8, 10]. These results were attributed to the presence of a compensation temperature (T_{comp}) at which the two collinear sublattice magnetizations M_{Tb} and M_{Co} compensate, which is above (resp. below) RT for $x = 30$ at.% (resp. $x = 16$ at.%). Therefore, such compensation temperature can only be reached through laser-induced heating for $x = 30$ at.% [7, 8]. For $x = 30$ at.%, AO-HDS is obtained at first in a rim at the edge of a demagnetized area and is then subsequently transferred to the scanned region leading to its total reversal. Moreover, other Tb dominated alloys with x ranging from 22 at.% to 27.5 at.% and t down to 4.5 nm show also AO-HDS, as can be seen from Fig. 2.

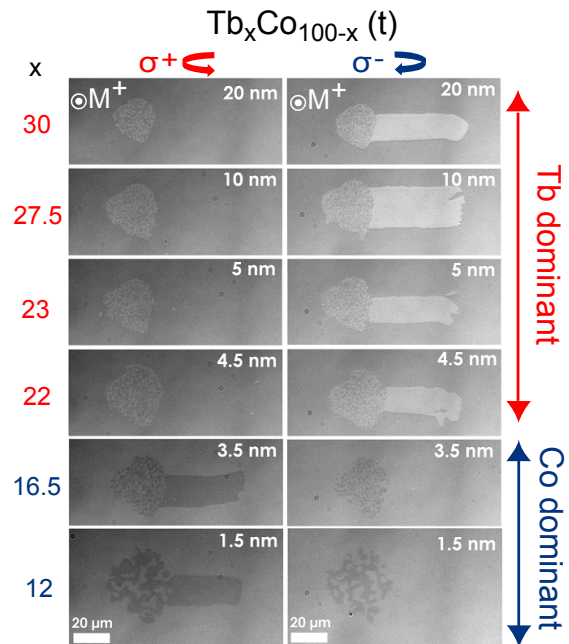


FIG. 2. Faraday imaging of $\text{Tb}_x\text{Co}_{100-x}$ (t) alloy films for Tb concentration x ranging from 12 to 30 and alloy thickness varying from 1.5 nm to 20 nm. For each sample, right- and left-circularly polarized laser beam were swept over the sample from right to left. The initial magnetization saturation up is exemplarily shown. The white contrast for the alloy thickness varying from 20 nm to 4.5 nm corresponds to a reversal to down, whereas the dark contrast for the alloy thickness 3.5 nm and 1.5 nm corresponds to a reversal to down.

For Co-dominated alloys, Fig. 1 shows that the signatures of the AO-HDS appear gradually by reducing the alloy thickness. For $t = 10$ nm and $x = 15.5$ at.%, the helicity dependence is slightly observed at the level of the AOS rim, whereas the laser-induced multiple magnetic domains get larger. For $t = 8$ nm and $x = 15$ at.%, AO-HDS is almost obtained with a presence of a small domain in the middle of the scanned region, whereas a complete AO-HDS is achieved for lower thicknesses $t \leq 6.5$ nm and Tb concentration ranging from 8 at.% to 16.5

at.% (see Figs. 1 and 2). The Co dominated $\text{Tb}_8\text{Co}_{92}$ (1.5 nm) shows pure AO-HDS, even if such alloy does not present a compensation above RT and has a high saturation magnetization and remanence $M_s = M_R = 830 \text{ emu/cm}^3$. These findings contradict the criterion of low remanence for the achievement of AO-HDS process [10], and also indicate that the magnetic film thickness plays an important role in such process.

Moreover, one can see from Figs. 1 and 2 that after initial magnetization saturation up, right- ($\sigma+$) (resp. left- ($\sigma-$)) circular polarized beam switches the magnetization to down for Co dominated (resp. Tb dominated) TbCo alloy films, which is attributed to the fact that the helicity of switching depends on the orientation of the Co sublattice magnetization and not on the direction of the net magnetization of the TbCo alloy film [19]. Furthermore, a demagnetized area is located to the left of the scanned region and is obtained when the beam is turned off, which is mainly attributed to demagnetization effects due to the cooling (see Figs. 1 and 2). One can clearly see that the size of magnetic domains in such demagnetized area increases for lower thicknesses, which is in agreement with previous studies [20].

B. Thickness-dependence of all-optical switching in ferromagnets

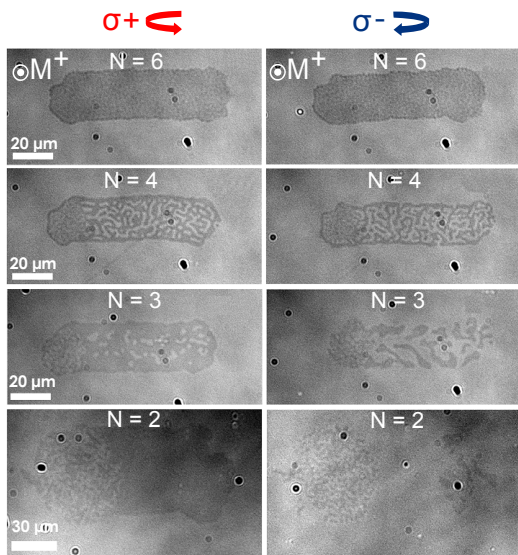


FIG. 3. Faraday imaging of $[\text{Co} (0.2 \text{ nm})/\text{Ni} (0.6 \text{ nm})]_N$ multilayers for number of repeats N ranging for 2 to 6. For each sample, right- and left-circularly polarized laser beam were swept over the sample from right to left. The initial magnetization saturation up is exemplarily shown. The dark contrast corresponds to a reversal to down.

As already mentioned, the recently discovered AO-HDS in Co/Pt multilayers with high saturation magne-

tization and no antiferromagnetic coupling between two sublattices [12] raises the question of what is the parameter limiting the achievement of AO-HDS and is it common to ferrimagnets as well as to ferromagnets? In this context, we have experimentally investigated the AO-HDS ability for two different ferromagnetic $[\text{Co}/\text{Ni}]_N$ and $[\text{Co}/\text{Pt}]_N$ multilayers by varying the number of repeats N . In regards to $[\text{Co}/\text{Ni}]_N$ multilayers, one can see from Fig. 3 that the signature of the AO-HDS starts to appear gradually by decreasing the number of repeats N and thus by decreasing the total magnetic thickness. Indeed, only TD is obtained for N ranging from 3 to 6, whereas a pure AO-HDS is achieved for $N = 2$. The size of the laser-induced multiple magnetic domains in the scanned area increases gradually by lowering N from 6 to 3, which suggests that the large domain size might also be an ingredient for obtaining the AO-HDS.

We also verified the AO-HDS ability in $[\text{Co}/\text{Pt}]_N$ multilayers and the result is consistent with the previous study of Lambert *et al.* [12]. As shown in Fig. 4, AO-HDS is achieved for $N = 1$ and 2 whereas only thermal demagnetization is obtained for $N = 3$ and 4 with larger domain size in the scanned region for $N = 3$. This switching ability for both Co/Pt and Co/Ni multilayers was maintained for a laser fluence ranging from the switching threshold to the damage threshold. Finally, one can conclude that the AO-HDS is achieved for both ferromagnetic Co/Ni and Co/Pt multilayers by reducing the magnetic thickness, a behavior which is similar to the one demonstrated in ferrimagnetic TbCo alloy films in Fig. 1.

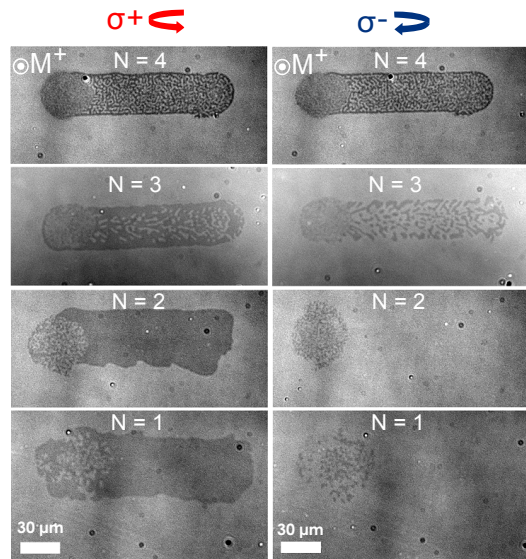


FIG. 4. Faraday imaging of $[\text{Pt} (0.7 \text{ nm})/\text{Co} (0.6 \text{ nm})]_N$ multilayers for number of repeats N ranging for 1 to 3. For each sample, right- and left-circularly polarized laser beam were swept over the sample from right to left. The initial magnetization saturation up is exemplarily shown. The dark contrast corresponds to a reversal to down.

C. Influence of magnetic domains in the observation of all-optical switching

The thickness-dependent investigation of AO-HDS in ferro- and ferri-magnets reveals that AO-HDS is observed when the magnetic film thickness is reduced. This behavior is common for both ferro- and ferri-magnets. To find a criterion which would allow predicting if AO-HDS will be observed or not, we compared the expected domain size due the competition between exchange, anisotropy and dipolar interaction to the size of the laser spot. Indeed, it is well known that the size of a stable magnetic domain in perpendicularly magnetized thin film is strongly dependent on the film thickness [21, 22]. This results from the competition between the dipolar energy that stabilizes small domains, and the domain wall energy that tends to reduce the length of the walls and so stabilizes big domains. It is therefore reasonable to infer that if the size of stable magnetic domains after the laser-induced heating is smaller than the size of the laser spot, TD will be observed because the system will break into small domains during cooling. On the contrary, if the magnetic domain size is larger than the size of the laser spot, AO-HDS can be observed. As a result, the magnetic domain size can be considered as a relevant predictive parameter for the observation of AO-HDS.

In order to estimate the domain size for the investigated ferro- and ferri-magnets, we use the model proposed by Kooy *et al.* [21] of periodic stripe domains with a strong uniaxial anisotropy in an infinite plate. We make the approximation that the domain wall size is negligible compared to the magnetic domain size and that the magnetization is perpendicular to the film plane within the domains. Thus, the magnetic domain size D that corresponds to the minimization of the total energy is expressed by:

$$D = t \exp \left[\frac{\pi D_0}{2t} + \ln \pi - 1 + \mu \left(\frac{1}{2} - \ln 2 \right) \right] \quad (1)$$

where $D_0 = \frac{\sigma}{E_d}$ is the dipolar length and $\mu = 1 + \frac{E_d}{K_u}$ is the magnetic susceptibility. $E_d = 2\pi M_s^2$ is the demagnetizing energy per unit volume, $\sigma = 4\sqrt{A_{\text{ex}} K_u}$ is the DW energy per unit surface, and t is the magnetic thickness.

As can be seen from Eq. (1), the material parameters involved in the calculation of the domain size are the saturation magnetization, the effective anisotropy and the exchange constant. An overview of the magnetic parameter values and the response to optical excitation for the studied films is presented in Table I. The saturation magnetization for all studied films and the effective anisotropy for $[\text{Co}/\text{Pt}]_N$ and $[\text{Co}/\text{Ni}]_N$ multilayers were measured with SQUID magnetometry, whereas the values of the effective anisotropy for $\text{Tb}_x\text{Co}_{100-x}$ (t) alloy films were deduced from the experimental data of Alebrand *et al.* [7]. The exchange constant A_{ex} for the investigated materials were estimated from literature data:

$A_{\text{ex}}(\text{Tb}_{27}\text{Co}_{30}) = 0.62 \cdot 10^{-6}$ erg/cm [23], $A_{\text{ex}}(\text{Co}/\text{Pt}) = 1.2 \cdot 10^{-6}$ erg/cm [24], $A_{\text{ex}}(\text{Co}/\text{Ni}) = 0.88 \cdot 10^{-6}$ erg/cm [25, 26]. As a first approximation, we suppose that the exchange constant A_{ex} is unchanged with Tb concentration and magnetic thickness t for $\text{Tb}_x\text{Co}_{100-x}$ (t) alloy films, since its variation with t is negligible compared to the variation of the other magnetic parameters. The Co/Pt multilayer is treated as a ferromagnetic single layer with thickness equal to the sum of Co layer thicknesses and magnetization worn only by the Co atoms. Therefore, due to the polarization of Pt, the saturation magnetization of $[\text{Co}/\text{Pt}]_N$ multilayers varies from 1483, 1609, 2194 to 2217 emu/cm³ for $N = 1, 2, 3$ and 4, respectively.

Furthermore, the conclusions on AO-HDS and the domain size extracted from this modeling remain the same if the Co/Pt multilayer is treated as a single ferromagnetic layer with a thickness equal to the total thickness of the multilayer and a magnetization equally distributed on the Co and Pt atoms (modeling made by Honda *et al.* [27]). However, in this case the domain wall energy is calculated only in the Co part of the multilayer (see Supplemental fig. 2).

We calculate the evolution of the domain size D as a function of the magnetic thickness t at RT for the investigated materials. Figure 5(a) shows the evolution of D for the two ferromagnets, whereas Figs. 5(b)-5(d) present such evolution for $\text{Tb}_x\text{Co}_{100-x}$ alloys for three different ranges of Tb concentration. For all the investigated materials, the divergence of D for low thickness t can be understood from Eq. (1) and is due to the decrease of the demagnetizing energy. In Fig. 5(a), four different curves of the domain size D are shown for $[\text{Co}/\text{Pt}]_N$ multilayers with N ranging from 1 to 4. This is due to the different values of M_s and K_u for each value of N , induced by the spin polarization of Pt atoms at the interfaces [17]. We define a domain size threshold $D_{th} = 50 \mu\text{m}$ corresponding to the size of the fs laser spot ($FWHM = 90 \mu\text{m}$).

One can see from Fig. 5(a) that for $[\text{Pt}(0.7)/\text{Co}(0.6)]_N$ multilayers with $N = 1$ ($t = 0.6$ nm) and $N = 2$ ($t = 1.2$ nm) which show AO-HDS, D is larger than D_{th} . While for $[\text{Pt}(0.7)/\text{Co}(0.6)]_N$ multilayers with $N > 3$ ($t > 1.8$ nm) which show TD, D is smaller than D_{th} . Moreover, for $[\text{Co}(0.2)/\text{Ni}(0.6)]_N$ multilayers $D > D_{th}$ only for $t < 2.4$ nm. Hence, the occurrence of AO-HDS for the investigated ferromagnets corresponds to a domain size at room temperature larger than the laser spot. During the AO-HDS process, the sample temperature will increase due to the laser-induced heating. Hence, we should also take into account the evolution of the domain size during cooling. In the case of ferromagnets, fs laser beam heats the magnetic system leading to a strong decrease of M_s [28]. Moreover, as can be understood from Eq. (1), the effect of the variation of K_u and A_{ex} on the domain size during cooling is low compared to the one of M_s . Due to the laser-induced decrease of M_s , the domain size during cooling for $[\text{Pt}(0.7)/\text{Co}(0.6)]_1$ and $[\text{Pt}(0.7)/\text{Co}(0.6)]_2$ is

Ferri- and ferro-magnets		t (nm)	M_s (emu/cm ³)	K_u ($\times 10^4$ erg/cm ³)	A_{ex} ($\times 10^{-6}$ erg/cm)	AOS vs TD
Tb _x Co _{100-x} (t)	x = 8	1.5	838	520	0.62	AOS
	x = 10.5	2.5	658	592	0.62	AOS
	x = 12	1.5	537	806	0.62	AOS
	x = 13.5	5	440	935	0.62	AOS
	x = 14.5	6.5	361	921	0.62	AOS
	x = 15	8	838	894	0.62	TD / AOS
	x = 15.5	10	308	893	0.62	TD
	x = 16	20	204	632	0.62	TD
	x = 16.5	3.5	230	725	0.62	AOS
	x = 25	6.5	183	503	0.62	AOS
	x = 27.5	10	298	641	0.62	AOS
	x = 30	20	341	678	0.62	AOS
	x = 30.5	15	360	432	0.62	AOS
[Co(0.6)/Pt(0.7)] _N	N = 1	0.6	1438	2650	1.2	AOS
	N = 2	1.2	1609	2472	1.2	AOS
	N = 3	1.8	2194	4162	1.2	TD / AOS
	N = 4	2.4	2217	4141	1.2	TD
[Co(0.2)/Ni(0.6)] _N	N = 2	1.6	1100	955	0.88	AOS
	N = 3	2.4	1100	955	0.88	TD / AOS
	N = 4	3.2	1100	955	0.88	TD
	N = 6	4.8	1100	955	0.88	TD

TABLE I. Overview of magnetic parameters for studied ferrimagnetic alloys and ferromagnetic multilayers for different values of Tb concentration x and magnetic thickness t . Saturation magnetization M_s was measured by SQUID magnetometry, whereas effective anisotropy K_u and exchange constant A_{ex} were estimated using data from literature [7, 13, 23–26].

always larger than D at RT, and therefore larger than the spot size D_{th} . For [Co/Pt]₃, let us consider that the sample has cooled down to a temperature of 400 K. We estimate the M_s at $T = 400$ K using the Curie-Weiss law with a Curie temperature $T_c = 650$ K, and we find $M_s = 1950$ emu/cm³. As can be seen from Fig. 6(a), the estimated domain size for [Pt(0.7)/Co(0.6)]₃ with $M_s = 1950$ emu/cm³ coincides with the spot size. Taking into account the decrease of K_u and A_{ex} at $T = 400$ K, it can be understood from Eq. (1) that the domains are always smaller than the spot size during cooling from 400 K to RT. Moreover, the domains are also smaller than D_{th} during cooling for [Pt(0.7)/Co(0.6)]₄. Consequently, we can conclude that the observation of a persistent switching for ferromagnets requires a domain size constantly larger than the spot size during cooling.

In order to demonstrate that such switching criterion is common for ferro- and ferri-magnets, we use the same approach to estimate the domain size during cooling for Tb_xCo_{100-x} (t) alloys for different ranges of Tb concentration x . It was demonstrated by Hansen *et al.* [29] for similar ferrimagnetic alloys that the saturation magnetization shows different behaviors with temperature de-

pending on the Tb concentration. Therefore, three different ranges of x can be distinguished, namely $8 < x < 13.5$, $14.5 < x < 16.5$ and $25 < x < 30.5$. The evolution of the domain size D at RT is studied on these three ranges as shown in Figs. 5(b), 5(c) and 5(d), respectively.

As can be seen from Fig. 5(b), for Tb_xCo_{100-x} (t) films showing AO-HDS with $x = 8, 10.5, 12, 13.5$ and $t = 1.5$ nm, 2.5 nm, 1.5 nm, 5 nm, respectively, D is larger than D_{th} at RT. For this range of concentration ($8 < x < 13.5$), M_s only decreases for $T > RT$ [29]. Hence, the domain size D during cooling for these materials which exhibit AO-HDS is always larger than D at RT, and thus larger than the spot size. For this range of Tb composition, the behavior of magnetic domains with temperature is really similar to the one in ferromagnets.

Concerning the range of Tb concentration $25 < x < 30.5$, for Tb₂₅Co₇₅ (6.5 nm), Tb_{27.5}Co_{72.5} (10 nm), Tb₃₀Co₇₀ (20 nm) and Tb_{30.5}Co_{69.5} (15 nm) showing AO-HDS, D is larger than D_{th} at RT as shown in Fig. 5(d). Moreover, Tb_xCo_{100-x} alloys for this range of concentration show a compensation temperature (T_{comp}) above room temperature [7, 29]. Hence, decreasing the temperature from the Curie temperature, M_s decreases

with temperature and vanishes at T_{comp} [7, 29]. The domains for these materials during cooling are therefore larger than those at RT, and thus larger than the spot size. A further decrease of temperature towards room temperature leads to an increase of M_s . However, since the nucleation is a thermally activated process and temperature is close to room temperature, the nucleation of new domains does not occur and AO-HDS is maintained.

A more tricky behavior is the one observed for the range of Tb concentration $14.5 < x < 16.5$. For $\text{Tb}_{14.5}\text{Co}_{85.5}$ (6.5 nm) and $\text{Tb}_{16.5}\text{Co}_{83.5}$ (3.5 nm) AO-HDS is observed, while for $\text{Tb}_{15}\text{Co}_{85}$ (8 nm), $\text{Tb}_{15.5}\text{Co}_{84.8}$ (10 nm) and $\text{Tb}_{16}\text{Co}_{84}$ (20 nm) only TD is obtained. However, the domain size for all these samples at RT is always larger than D_{th} as can be seen from Fig. 5(c). Nevertheless, the saturation magnetization increases with temperature ($\text{RT} < T < 500 \text{ K}$) for this

range of concentration [29]. For instance, an increase in M_s by 150 emu/cm^3 is estimated for $\text{Tb}_{16}\text{Co}_{84}$ (20 nm) at $T = 500 \text{ K}$. Taking into account the decrease of K_u with temperature, the domains in $\text{Tb}_{16}\text{Co}_{84}$ (20 nm) are smaller than the spot size at $T = 500 \text{ K}$ (see Fig. 6(b)). Hence, for $\text{Tb}_{16}\text{Co}_{84}$ (20 nm), $\text{Tb}_{15}\text{Co}_{85}$ (8 nm) and $\text{Tb}_{15.5}\text{Co}_{84.8}$ (10 nm) which show TD, the domains get smaller than the spot size during cooling thus canceling the initial effect of the helicity. Furthermore, for $\text{Tb}_{14.5}\text{Co}_{85.5}$ (6.5 nm) and $\text{Tb}_{16.5}\text{Co}_{83.5}$ (3.5 nm) showing AO-HDS, the domain size during cooling is smaller than the one at RT, but remains larger than the spot size despite an increase in M_s by 150 emu/cm^3 . A domain size larger than the spot size during cooling is therefore required to achieve the switching for this range of Tb concentration.

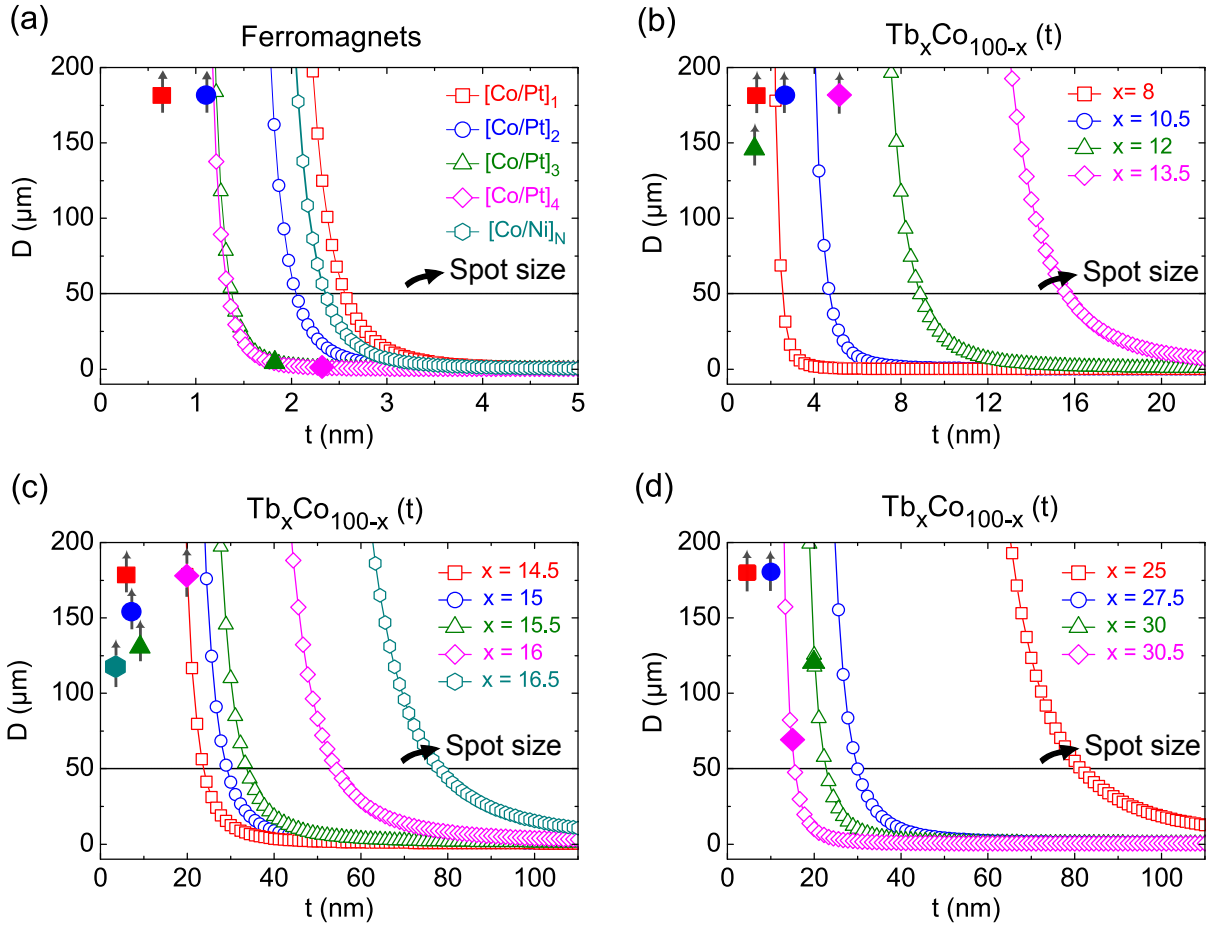


FIG. 5. Estimation of the magnetic domain size D as a function of the magnetic thickness t at room temperature for the studied ferro- and ferri-magnets. (a) $[\text{Pt}(0.7 \text{ nm})/\text{Co}(0.6 \text{ nm})]_N$ and $[\text{Co}(0.2 \text{ nm})/\text{Ni}(0.6 \text{ nm})]_N$ multilayers. (b) $\text{Tb}_x\text{Co}_{100-x}$ alloys for x ranging from 8 to 13.5. (c) $\text{Tb}_x\text{Co}_{100-x}$ alloys for x ranging from 14.5 to 16.5. (d) $\text{Tb}_x\text{Co}_{100-x}$ alloys for x ranging from 25 to 30.5. The filled symbols indicate the magnetic thickness of the investigated ferro- and ferri-magnets.

Consequently, a domain size larger than the spot size during cooling is required to achieve a persistent all-

optical switching, which is easier to fulfill by decreasing the magnetic film thickness. This criterion is common for

both investigated ferro- and ferri-magnets and could also be satisfied by strongly decreasing the spot size below the domain size at RT. However, a significant decrease of the size of the 35-fs laser spot is difficult to achieve with our experimental set up due to the diffraction limits.

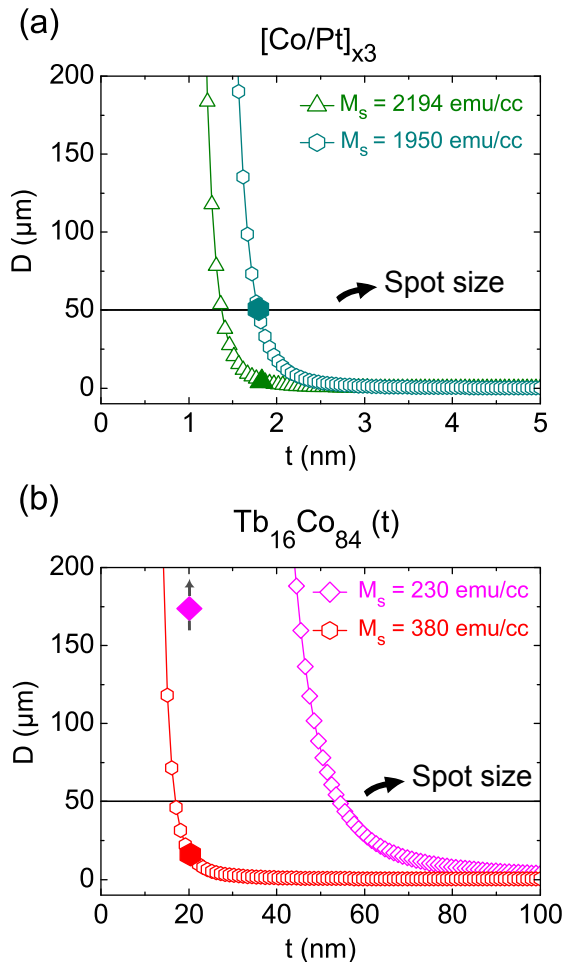


FIG. 6. (a) Estimation of the domain size D as a function the magnetic thickness t for $[\text{Pt}(0.7 \text{ nm})/\text{Co}(0.6 \text{ nm})]_3$ multilayers for $M_s = 2194 \text{ emu/cm}^3$ measured at RT and $M_s = 1950 \text{ emu/cm}^3$ calculated at $T = 400 \text{ K}$. For $t = 1.8 \text{ nm}$ with $M_s = 1950 \text{ emu/cm}^3$, the domain size coincides with the laser spot size. (b) Estimation of D as a function of t for $\text{Tb}_{16}\text{Co}_{84}(t)$ alloys for $M_s = 230 \text{ emu/cm}^3$ measured at RT and $M_s = 380 \text{ emu/cm}^3$ estimated at $T = 500 \text{ K}$. For $t = 20 \text{ nm}$ with $M_s = 380 \text{ emu/cm}^3$, the domain size is smaller than the laser spot size. The filled symbols indicate the magnetic thickness of the investigated ferro- and ferri-magnets.

IV. CONCLUSION

In conclusion, we have experimentally investigated the thickness-dependence of the AO-HDS in ferromagnetic Co/Pt and Co/Ni multilayers as well as ferrimagnetic

TbCo alloys with different concentrations. For instance, we demonstrated that both ferro- and ferri-magnets with high saturation magnetization ($M_s > 700 \text{ emu/cm}^3$) show a persistent switching if the magnetic thickness is strongly reduced. We could define a common criterion to predict the observation of AO-HDS. Indeed, after the circularly polarized laser pulses heat the perpendicularly magnetized sample, the magnetization tends to break into domains while cooling down. Hence, if the magnetic domain size inside the material during the cooling process is larger than the laser spot size then AO-HDS can be observed, otherwise thermal demagnetization will be seen. Such criterion for the observation of AO-HDS is common for both investigated ferro- and ferri-magnets. From a phenomenological point of view, we suspect that much more magnetic materials are expected to show AO-HDS, but the initial effect of the helicity is canceled by the formation of small magnetic domains during the cooling process. From a technological point of view, this decisive role of magnetic domains allows identifying the optimal conditions for the observation of a persistent AO-HDS, whether by significantly reducing the magnetic thickness to get larger domain size or by strongly decreasing the laser spot size in order to fulfill the criterion of a domain size constantly larger than the laser spot size during cooling.

ACKNOWLEDGMENTS

This work was supported by the ANR-NSF Project, ANR-13-IS04-0008-01, "COMAG" by the ANR-Labcom Project LSTNM, by the European Project (OP2M FP7-

IOF-2011-298060) and by the Université de la Grande Région (UniGR funded P. Pirro Post-Doc). Experiments were performed using equipment from the TUBE - Daum funded by FEDER (EU), ANR, the Region Lorraine and Grand Nancy.

-
- [1] E. Beaurepaire, J.C. Merle, A. Daunois, and J.Y. Bigot, *Phys. Rev. Lett.* 76, 4250-4253 (1996).
- [2] C. D. Stanciu, F. Hansteen, A. V. Kimel, A. Kirilyuk, A. Tsukamoto, A. Itoh, and T. Rasing, *Phys. Rev. Lett.* 99, 047601 (2007).
- [3] A. Kirilyuk, A. V. Kimel, and T. Rasing, *Rev. Mod. Phys.* 82, 27312784 (2010).
- [4] I. Radu, K. Vahaplar, C. Stamm, T. Kachel, N. Pontius, H. A. Durr, T. A. Ostler, J. Barker, R. F. Evans, R. W. Chantrell, A. Tsukamoto, A. Itoh, A. Kirilyuk, Th. Rasing, and A. V. Kimel, *Nature* 472, 205208 (2011).
- [5] T. A. Ostler, J. Barker, R. F. L. Evans, R. W. Chantrell, U. Atxitia, O. Chubykalo-Fesenko, S. El Moussaoui, L. Le Guyader, E. Mengotti, L. J. Heyderman, F. Nolting, A. Tsukamoto, A. Itoh, D. Afanasiev, B.A. Ivanov, A.M. Kalashnikova, K. Vahaplar, J. Mentink, A. Kirilyuk, Th. Rasing, and A.V. Kimel, *Nat. Commun.* 3, 666 (2012).
- [6] A. R. Khorsand, M. Savoini, A. Kirilyuk, A. V. Kimel, A. Tsukamoto, A. Itoh, and T. Rasing, *Phys. Rev. Lett.* 108, 127205 (2012).
- [7] S. Alebrand, M. Gottwald, M. Hehn, D. Steil, M. Cinchetti, D. Lacour, E.E. Fullerton, M. Aeschlimann, and S. Mangin, *Appl. Phys. Lett.* 101, 162408 (2012).
- [8] S. Mangin, M. Gottwald, C.-H. Lambert, D. Steil, V. Uhlir, L. Pang, M. Hehn, S. Alebrand, M. Cinchetti, G. Malinowski, Y. Fainman, M. Aeschlimann, and E. E. Fullerton, *Nat. Mater.* 13, 286292 (2014).
- [9] A. V. Kimel, *Nat. Mater.* 13, 225226 (2014).
- [10] A. Hassdenteufel, J. Schmidt, C. Schubert, B. Hebler, M. Helm, M. Albrecht, and R. Bratschitsch, *Phys. Rev. B* 91, 104431 (2015).
- [11] B. Hebler, A. Hassdenteufel, P. Reinhardt, H. Karl, and M. Albrecht, *Front. Mater.* 3:8 (2016).
- [12] C. H. Lambert, S. Mangin, B. S. D. C. S. Varaprasad, Y. K. Takahashi, M. Hehn, M. Cinchetti, G. Malinowski, K. Hono, Y. Fainman, M. Aeschlimann, and E. E. Fullerton, *Science* 345, 13371340 (2014).
- [13] M. S. El Hadri, P. Pirro, C.-H. Lambert, N. Bergeard, S. Petit-Watelot, M. Hehn, G. Malinowski, F. Montaigne, Y. Quessab, R. Medapalli, E. E. Fullerton, and S. Mangin, *Appl. Phys. Lett.* 108, 092405 (2016).
- [14] R. Malmhall, and T. Chen, *J. Appl. Phys.* 53, 7843 (1982).
- [15] D. H. Shen, Y. Mizokawa, H. Iwasaki, D. F. Shen, T. Numata, and S. Nakamura, *Jpn. J. Appl. Phys.* 20, 757760 (1982).
- [16] M. T. Johnson, J. J. de Vries, N. W. E. McGee, J. aan de Stegge, and F. J. A. den Broeder, *Phys. Rev. Lett.* 69, 3575 (1992).
- [17] J. W. Knepper and F. Y. Yang, *Phys. Rev. B* 71, 224403 (2005).
- [18] M. S. El Hadri, P. Pirro, C.-H. Lambert, S. Petit-Watelot, Y. Quessab, M. Hehn, F. Montaigne, G. Malinowski, and S. Mangin, arXiv: 1602.08525 (2016).
- [19] A. Hassdenteufel, C. Schubert, J. Schmidt, P. Richter, D. R. T. Zahn, G. Salvan, M. Helm, R. Bratschitsch, and M. Albrecht, *Appl. Phys. Lett.* 105, 112403 (2014).
- [20] O. Hellwig, A. Berger, J.B. Kortright, and E.E. Fullerton, *J. Magn. Magn. Mater.* 319 (1-2), 13-55 (2007).
- [21] C. Kooy and U. Enz, *Philips Res. Repts.* 15, 7 (1960).
- [22] C. Kittel, *Phys. Rev.* 70, 965 (1946).
- [23] M. Gottwald, Ph.D. Thesis, Université Henri Poincaré (2011).
- [24] C. Eyrych, W. Huttema, M. Arora, E. Montoya, F. Rashidi, C. Burrowes, B. Kardasz, E. Girt, B. Heinrich, O. N. Mryasov, M. From, and O. Karis, *J. Appl. Phys.* 111, 07C919 (2012).
- [25] P. E. Tannenwald, *Phys. Rev.* 121, 715 (1961).
- [26] D. H. Martin, *Magnetism in Solids*, Iliffe Books Ltd., London, 1967, p. 67.
- [27] S. Honda, Y. Ikegawa and T. Kusuda, *J. Magn. Magn. Mater.* 111, 273-292 (1992).
- [28] D. J. Dunlop and . zdemir, *Rock Magnetism*, Cambridge studies in magnetism, Cambridge, 1997, p. 52.
- [29] P. Hansen, C. Clausen, G. Much, M. Rosenkranz, and K. Witter, *J. Appl. Phys.* 66, 756 (1989).